

## Review Article

# Synthesis of Organic Nanofibers with Embedded Palladium Nanoparticles for Decolourization of Organic Dyes

Bera T and Fang JY\*

Department of Materials Science and Engineering,  
University of Central Florida, USA**\*Corresponding author:** Fang JY, Department of  
Materials Science and Engineering, University of Central  
Florida, Orlando, Florida 32816, USA**Received:** May 16, 2014; **Accepted:** July 09, 2014;**Published:** July 14, 2014**Abstract**

We report the synthesis of organic nanofibers with embedded palladium nanoparticle (PdNP) by the self-assembly of Pd<sup>2+</sup>-coordinated lithocholic acid (LCA) in the presence of sodium borohydride (NaBH<sub>4</sub>) or ascorbic acid (AA) reducing agents. The *in-situ* reduction of Pd<sup>2+</sup> ions by NaBH<sub>4</sub> or AA leads to the formation of PdNPs in the interior of self-assembled LCA nanofibers. The catalytic activity of LCA nanofibers with embedded PdNPs in the decolourization of 4-phenyl azo benzoic acid (4-PABA) is investigated.

**Keywords:** Lithocholic acid; Self-assembly; Palladium nanoparticles; Nanofibers; Recyclable nanocatalysts

**Abbreviations**

LCA: Lithocholic Acid; PdNP: Palladium Nanoparticle; NaBH<sub>4</sub>: Sodium Borohydride; AA: Ascorbic Acid; 4-PABA: 4-phenyl Azo Benzoic acid

**Introduction**

There has been great interest in metal nanoparticles due to their applications as efficient nanocatalysts for chemical productions, energy processes, and pollution controls [1-3]. It is known that small metal nanoparticles are thermodynamically unstable. The aggregation of metal nanoparticles can lead to the reduction of their catalytic activities. Thus, surfactants are often used as a stabilizing agent for synthesizing metal nanoparticles [4-13]. However, the recyclability of surfactant-stabilized small metal nanoparticles still remains to be a challenge because they are difficult to be separated and recovered from reaction solution. Recently, efforts have been made for synthesizing one-dimensional metal nanostructures [14-17] or constructing metal nanoparticles on polymer nanofibers [18-21] in order to achieve the good recyclability.

Contrary to the commonly used surfactants in stabilizing metal nanoparticles, a number of lipids and bile acids can self-assemble into one-dimensional (1D) nanostructures with well-defined sizes and morphologies including fibers, ribbons and tubes [22-24]. These 1D nanostructures are promise as organized templates for growing and patterning inorganic nanoparticles [25-33]. The self-assembly of metal ion-coordinated lipids has been proven to an efficient method in the synthesis of metal ion-coordinated nanotubes [34-36]. The Cu ion- and Ni ion-coordinated lipid nanotubes have shown good catalytic activities for the effective oxidation of organic compounds [35-36].

Lithocholic acid (LCA) is a secondary bile acid. It has a rigid, nearly planar steroid nucleus and a short alkyl chain with a carboxyl terminal group. It has been shown that LCA can self-assemble in aqueous solution into helical ribbons and tubes [37-43], depending

on the experimental conditions under which self-assembly occurs. In a previous publication [43], we reported the formation of PdNP-LCA hybrid nanofibers by the self-assembly of Pd<sup>2+</sup>-coordinated LCA molecules, followed by an *ex-situ* reduction with sodium borohydride (NaBH<sub>4</sub>) or ascorbic acid (AA), in which PdNPs grow on the surface of the self-assembled LCA nanofibers [44]. In this paper, we report the synthesis of hybrid nanofibers by the self-assembly of Pd<sup>2+</sup>-coordinated LCA molecules in the presence of NaBH<sub>4</sub> or AA. The *in-situ* reduction by NaBH<sub>4</sub> or AA can lead to the formation of LCA nanofibers with embedded PdNPs. Azo dyes are widely used in the textile, pharmaceutical, food and cosmetics industries. They are one of primary sources to cause water pollution. The decolourization of organic dyes in water is critical in improving the quality of water. As a proof-of-concept, 4-phenyl azo benzoic acid (4-PABA) is chosen as a model dye. We demonstrate that LCA nanofibers with embedded PdNPs can be used as a recyclable nanocatalyst for the decolourization of 4-PABA in water.

**Experimental section**

Lithocholic acid (LCA), 4-phenyl azo benzoic acid (4-PABA), ammonium hydroxide (NH<sub>4</sub>OH), palladium chloride (PdCl<sub>2</sub>), ascorbic acid (AA), and sodium borohydride (NaBH<sub>4</sub>) were purchased from Sigma-Aldrich. Pd<sup>2+</sup>(NH<sub>4</sub>OH)<sub>6</sub>Cl<sub>2</sub> used as a precursor for the synthesis of PdNPs was prepared by dissolving PdCl<sub>2</sub> in NH<sub>4</sub>OH aqueous solution. NaBH<sub>4</sub> and AA were used as reducing agents. Water used in our experiments was purified with Easy pure II system (18MΩ cm, pH 5.7). Carbon-coated copper grids were purchased from Electron Microscopy Science.

Transmission electron microscopy (TEM) was performed with a JEOL1011-EM microscope operating at an acceleration voltage of 100 kV. Ultraviolet-visible (UV-vis) spectra were recorded using a Cary300 spectrophotometer. X-ray diffraction (XRD) measurements were carried out with a Rigaku D/max diffractometer with CuKα radiation (λ = 1.542 Å) operated at 40 kV and 30 mA.

**Results and Discussion**

The chemical structures of LCA and 4-PABA are shown in Figure 1. In our experiments, 30 mg of LCA was dissolved in 4mL of 0.01 M  $\text{NH}_4\text{OH}$  aqueous solution at pH 11.0. The pre-prepared  $\text{Pd}^{2+}(\text{NH}_4\text{OH})_6\text{Cl}_2$  solution was then added into 20mM LCA solution. The concentration of  $\text{Pd}^{2+}$  ions in the mixed solution varied from 0.1mM to 1mM. The mixed solution was stirred, followed by adding 400 $\mu\text{L}$  of 100mM of  $\text{NaBH}_4$  solution. Finally, the solution was vigorously stirred for 60 min and then sealed in a glass vial at room temperature. Figure 2a shows a low-resolution TEM image of nanofibers formed at the  $\text{Pd}^{2+}$  ion concentration of 1mM. The nanofibers are over 100  $\mu\text{m}$  long with diameters in the range from 70 nm to 180 nm. As can be seen from the high-resolution TEM image (Figure 2b), PdNPs (dark dots) with a diameter of 30-40 nm are embedded in the LCA nanofibers. In the synthesis process, the deprotonated LCA molecules provide negatively charged  $\text{COO}^-$  groups to coordinate with positively charged  $\text{Pd}^{2+}$  ions. The  $\text{Pd}^{2+}$ -coordinated LCA molecules then self-assemble into nanofibers in the presence of  $\text{NaBH}_4$  reducing agent. The formation of PdNPs inside the LCA nanofibers suggests that the coordinated  $\text{Pd}^{2+}$  ions

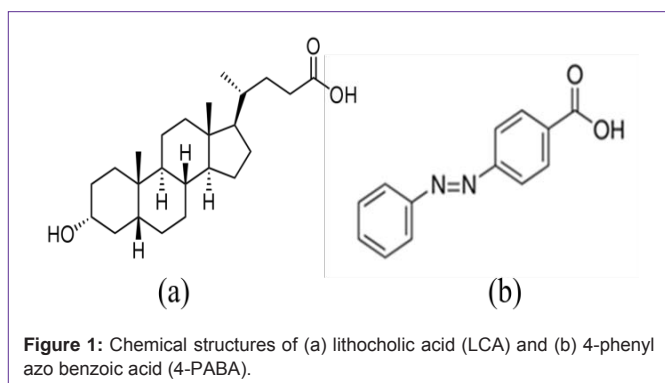


**Figure 1:** Chemical structures of (a) lithocholic acid (LCA) and (b) 4-phenyl azo benzoic acid (4-PABA).

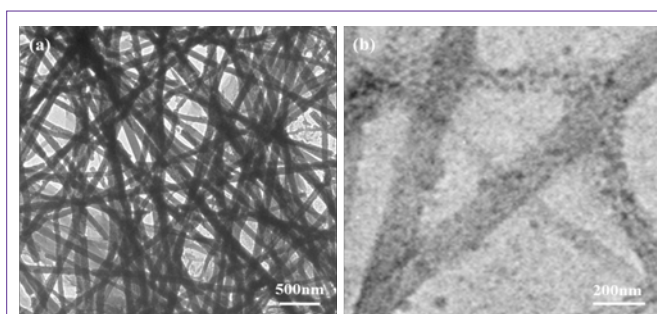


**Figure 2:** (a) Low and (b) high resolution TEM images of LCA nanofibers with embedded PdNPs.

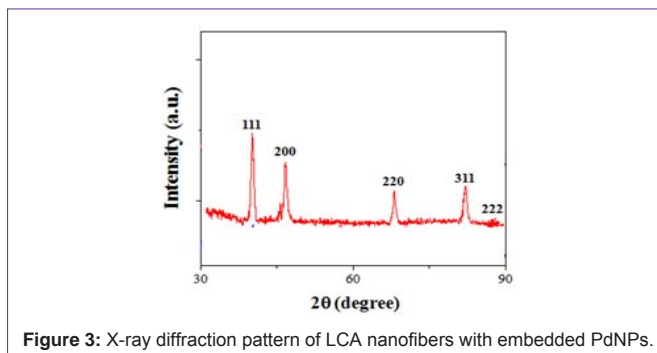


**Figure 3:** X-ray diffraction pattern of LCA nanofibers with embedded PdNPs.

are *in situ* reduced by  $\text{NaBH}_4$  to form Pd nuclei, which then grow into PdNPs inside the LCA nanofibers. X-ray diffraction patterns of LCA nanofibers with embedded PdNPs show five characteristic peaks (Figure 3), corresponding to the scattering from the (111), (200), (220), (311), and (222) planes of the face centered cubic PdNPs.

We studied the catalytic activity of LCA nanofibers with embedded PdNPs in the decolorization of 4-PABA in water. In our experiments, the LCA nanofibers with embedded PdNPs were purified by centrifugation to remove excess LCA and small PdNP-LCA aggregates. When 25 $\mu\text{L}$  of 10mM  $\text{NaBH}_4$  solution was added into 1mL of 1mM 4-PABA solution, we observe no color change, suggesting that the oxidation of 4-PABA proceeds at a very slow rate without catalysts. The addition of 25  $\mu\text{L}$  nanofiber solution causes the ultimate fading of the orange color of 4-PABA solution, suggesting that the LCA nanofibers with embedded PdNPs are able to effectively catalyze the decolorization reaction of 4-PABA. To quantitatively compare the catalytic activity of LCA nanofibers with embedded PdNPs formed at different conditions, we study the kinetics of the decolorization reaction by monitoring the reaction solution with UV-vis absorption spectroscopy as a function of time at room temperature. Figure 4a shows the time-resolved UV-vis absorption spectra of the decolorization of 4-PABA by the LCA nanofibers with embedded PdNPs synthesized at the  $\text{Pd}^{2+}$  concentration of 1mM, where  $\text{NaBH}_4$  was used as a reducing agent. The UV-vis absorption spectra were recorded in every 1 min. In the absence of the nanofibers, 4-PABA solution shows a characteristic absorption peak at 430 nm arising from the  $-\text{N}=\text{N}-$  bond of 4-PABA. The adsorption peak quickly decreases over time after the addition of LCA nanofibers with embedded PdNPs, suggesting that the nanofibers are capable of catalyzing the breakage of the  $-\text{N}=\text{N}-$  bond. After 10 min, the absorption peak at 430 nm disappears. Thus, we used the intensity of the absorption peak to quantitatively evaluate the catalytic performance of LCA nanofibers with embedded PdNPs. Figure 4b shows the plots of  $\ln(A_t/A_0)$  versus reaction time  $t$  for the decolorization of 4-PABA, where  $A_t$  and  $A_0$  is the intensity of absorption peaks at time  $t$  and 0, respectively. The linear relationship shown in Figure 4b suggests that the decolorization process by LCA nanofibers with embedded PdNPs follows pseudo-first-order kinetics. Since the concentration of  $\text{NaBH}_4$  is high, we expect that it remains essentially constant during the reaction. Thus, the pseudo-first-order kinetics can be used to evaluate the catalytic rate of LCA nanofibers with embedded PdNPs in the decolorization of 4-PABA. The rate constant calculated from the slope of the plot shown in Figure 4b is  $3.04 \times 10^{-4} \text{ s}^{-1}$ . The pseudo-first-order kinetics is also observed if AA is used as a reducing agent (Figure 4c). In this case, the calculated rate constant is  $1.08 \times 10^{-4} \text{ s}^{-1}$ . The reduced rate constant is because AA is a weaker reducing agent, compared to  $\text{NaBH}_4$ .

Furthermore, we study the catalytic performance of LCA nanofibers with embedded PdNPs synthesized at different  $\text{Pd}^{2+}$  concentrations. Figure 5a shows the plots of  $\ln(A_t/A_0)$  versus reaction time  $t$  for the decolorization of 4-PABA, in which  $\text{NaBH}_4$  was used as a reducing agent. As can be seen in Figure 5b, all the decolorization processes show pseudo-first-order kinetics. The rate constant decreases from  $3.45 \times 10^{-4} \text{ s}^{-1}$  to  $0.59 \times 10^{-4} \text{ s}^{-1}$  when the  $\text{Pd}^{2+}$  concentration decreases from 1mM to 0.1mM.

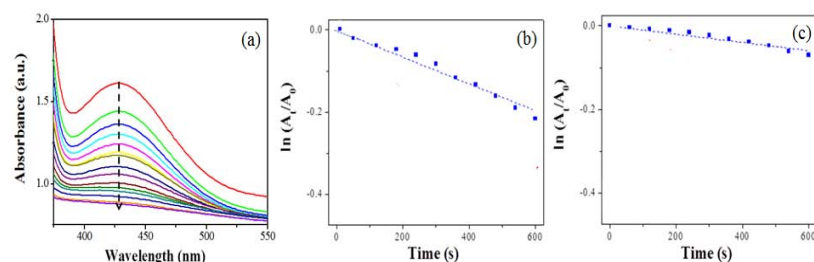


**Figure 4:** (a) Time-resolved UV-vis absorption spectra for the decolorization of 4-PABA by LCA nanofibers with embedded PdNPs. The spectra were recorded every 1 min. Plots of  $\ln(A_t/A_0)$  versus time for the decolorization of 4-PABA by the LCA nanofibers with embedded PdNPs in the presence of  $\text{NaBH}_4$  (b) and AA (c).

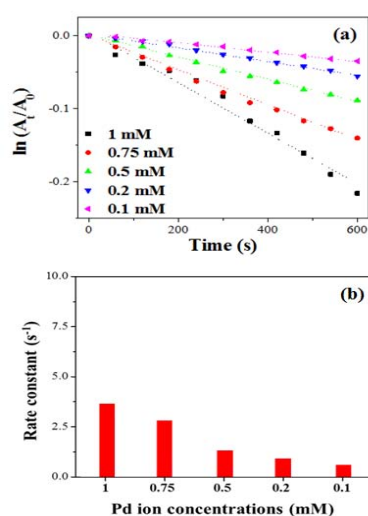


**Figure 5:** (a) Plots of  $\ln(A_t/A_0)$  versus time for the decolorization of 4-PABA by LCA nanofibers with embedded PdNPs synthesized in different  $\text{Pd}^{2+}$  concentrations, in which  $\text{NaBH}_4$  was used as a reducing agent. (b) Rate constants versus  $\text{Pd}^{2+}$  ion concentrations.

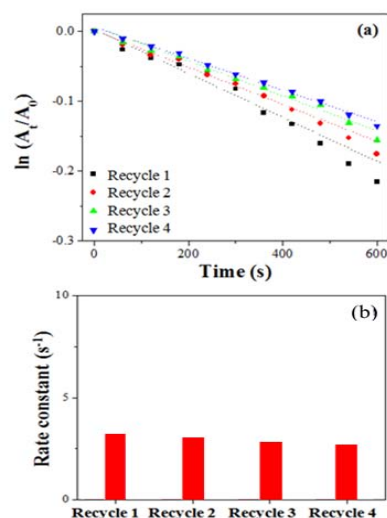


**Figure 6:** (a) Plots of  $\ln(A_t/A_0)$  versus time for the decolorization of 4-PABA by LCA nanofibers with embedded PdNPs for four recycles. (b) Rate constants versus recycles.

One of the advantages of using LCA nanofibers with embedded PdNPs as a nanocatalyst is that they can be easily separated and recovered from reaction solution due to their high aspect ratios. After each reaction cycle, LCA nanofibers were recovered from the reaction solution by centrifugation. Figure 6a shows the plots of  $\ln(A_t/A_0)$  versus reaction time  $t$  for the decolorization of 4-PABA by LCA nanofibers with embedded PdNPs for four recycling tests, where  $\text{NaBH}_4$  is used as a reducing agent. As can be seen from Figure 6b, the decolorization processes of each recycle shows pseudo-first-order kinetics. The rate constant shows only a slight decrease from  $3.04 \times 10^{-4} \text{ s}^{-1}$  to  $2.31 \times 10^{-4} \text{ s}^{-1}$ .

## Conclusion

We report the synthesis of organic nanofibers with embedded PdNPs by the self-assembly of  $\text{Pd}^{2+}$ -coordinated LCA molecules and an *in-situ* reduction approach. The LCA nanofibers with embedded PdNPs show good catalytic activity in the decolorization of 4-PABA by using  $\text{NaBH}_4$  or AA as a reducing agent. We demonstrate that the LCA nanofibers with embedded PdNPs can be used as a recyclable nanocatalyst for the decolorization of 4-PABA in water.

## Acknowledgment

This work was supported by the National Science Foundation (CBET 0855322).

## References

- Roucoux A, Schulz J, Patin H. Reduced transition metal colloids: a novel family of reusable catalysts? *Chem Rev.* 2002; 102: 3757-3778.
- Astruc D, Lu F, Aranzues JR. Nanoparticles as recyclable catalysts: the frontier between homogeneous and heterogeneous catalysis. *Angew Chem Int Ed Engl.* 2005; 44: 7852-7872.
- Climent MJ, Corma A, Iborra S. Heterogeneous catalysts for the one-pot synthesis of chemicals and fine chemicals. *Chem Rev.* 2011; 111: 1072-1133.
- Klingelhöfer S, Heitz W, Greiner A, Oestreich S, Förster S, Antonietti M. Preparation of palladium colloids in block copolymer micelles and their use for the catalysis of the heck reaction. *J. Am. Chem. Soc.* 1997; 119: 10116-10120.
- Henglein A, Ershov BG, Malow M. Absorption spectrum and some chemical reactions of colloidal platinum in aqueous solution. *J. Phys. Chem.* 1995; 99: 14129-14136.
- Ohde H, Wai CM, Kim H, Kim J, Ohde M. Hydrogenation of olefins in supercritical  $\text{CO}_2$  catalyzed by palladium nanoparticles in a water-in- $\text{CO}_2$  microemulsion. *J Am Chem Soc.* 2002; 124: 4540-4541.
- Yoon B, Kim H, Wai CM. Dispersing palladium nanoparticles using a water-in-oil microemulsion—homogenization of heterogeneous catalysis. *Chem*

- Commun (Camb). 2003; 1040-1041.
- Meric P, Yu KM, Tsang SC. Micelle-hosted palladium nanoparticles catalyze citral molecule hydrogenation in supercritical carbon dioxide. *Langmuir*. 2004; 20: 8537-8545.
  - Liu J, Alvarez J, Ong W, Roman E, Kaifer AE. Tuning the catalytic activity of cyclodextrin-modified palladium nanoparticles through host-guest binding interactions. *Langmuir*. 2001; 17: 6762-6764.
  - Lee CL, Wan CC, Wang YY. Synthesis of metal nanoparticles via self-regulated reduction by an alcohol surfactant. *Adv. Funct. Mater.* 2001; 11: 344-347.
  - Ibañez FJ, Zamborini FP. Reactivity of hydrogen with solid-state films of alkylamine- and tetraoctylammonium bromide-stabilized Pd, PdAg, and PdAu nanoparticles for sensing and catalysis applications. *J Am Chem Soc*. 2008; 130: 622-633.
  - Sadeghmoghaddam E, Lam C, Choi D, Shon YS. Synthesis and catalytic properties of alkanethiolate-capped Pd nanoparticles generated from sodium S-dodecylthiosulfate. *J. Mater. Chem.* 2011; 21: 307-312.
  - Moreno M, Ibañez FJ, Jasinski JB, Zamborini FP. Hydrogen reactivity of palladium nanoparticles coated with mixed monolayers of alkyl thiols and alkyl amines for sensing and catalysis applications. *J Am Chem Soc*. 2011; 133: 4389-4397.
  - Chen Z, Waje M, Li W, Yan Y. Supportless Pt and PtPd nanotubes as electrocatalysts for oxygen-reduction reactions. *Angew Chem Int Ed Engl*. 2007; 46: 4060-4063.
  - Zhou HJ, Zhou WP, Adzic RR, Wong SS. Enhanced electrocatalytic performance of one-dimensional metal nanowires and arrays generated via an ambient, surfactantless synthesis. *J. Phys. Chem. C*. 2009; 113: 5460-5466.
  - Lim B, Xia Y. Metal nanocrystals with highly branched morphologies. *Angew Chem Int Ed Engl*. 2011; 50: 76-85.
  - Niu Z, Wang D, Yu R, Peng Q, Li Y. Highly branched Pt-Ni nanocrystals enclosed by stepped surface for methanol oxidation. *Chem. Sci.* 2012; 3: 1925-1929.
  - Demir MM, Gulgun MA, Menciloglu YZ, Erman B, Abramchuk SS, Makhaeva EE, et al. Palladium nanoparticles by electrospinning from poly (acrylonitrile-co-acrylic acid)-PdCl<sub>2</sub> solutions. Relations between preparation conditions, particle size, and catalytic activity. *Macromolecules* 2004; 37: 1787-1792.
  - Fang X, Ma H, Xiao S, Shen M, Guo R, Cao X, et al. Facile immobilization of gold nanoparticles into electrospun polyethyleneimine/polyvinyl alcohol nanofibers for catalytic applications. *J. Mater. Chem.* 2011; 21: 4493-4501.
  - Ma H, Huang Y, Shen M, Hu D, Yang H, Zhu M, et al. Enhanced decoloration efficacy of electrospun polymer nanofibers immobilized with Fe/Ni bimetallic nanoparticles. *RSC Adv.* 2013; 3: 6455-6465.
  - Cao M, Zhou L, Xu X, Cheng S, Yao JL, Fan LJ. Galvanic replacement approach for bifunctional polyacrylonitrile/Ag-M (M = Au or Pd) nanofibers as SERS-active substrates for monitoring catalytic reactions. *J. Mater. Chem. A* 2013; 1: 8942-8949.
  - Shimizu T, Masuda M, Minamikawa H. Supramolecular nanotube architectures based on amphiphilic molecules. *Chem Rev*. 2005; 105: 1401-1443.
  - Fang JY. Ordered arrays of self-assembled lipid tubules: fabrication and applications. *J. Mater. Chem.* 2007; 17: 3479-3784.
  - Guo L, Chowdhury P, Fang J, Gai F. Heterogeneous and anomalous diffusion inside lipid tubules. *J Phys Chem B*. 2007; 111: 14244-14249.
  - Burkett SL, Mann S. Spatial organization and patterning of gold nanoparticles on self-assembled biolipid tubular templates. *Chem. Commun.* 1996; 321-322.
  - Lvov YM, Price RR, Selinger JV, Singh A, Spector MS, Schnur JM. Imaging nanoscale patterns on biologically derived microstructures. *Langmuir*. 2000; 16: 5932-5935.
  - Banerjee IA, Yu L, Matsui H. Cu nanocrystal growth on peptide nanotubes by biomineralization: size control of Cu nanocrystals by tuning peptide conformation. *Proc Natl Acad Sci U S A*. 2003; 100: 14678-14682.
  - Banerjee A, Yu L, Matsui H. Location-specific biological functionalization on nanotubes: attachment of proteins at the ends of nanotubes using Au nanocrystal masks. *Nano Lett*. 2003; 3: 283-287.
  - Jung JH, Rim JA, Lee SJ, Lee SS. Spatial organization and patterning of palladium nanoparticles on a self-assembled helical ribbon lipid. *Chem. Commun.* 2005; 468-470.
  - Terech P, Sangeeth NM, Bhat S, Allegraud JJ, Buhler E. Ammonium lithocholate nanotubes: stability and copper metallization. *Soft Matt*. 2006; 2: 517-522.
  - Park C, Im MS, Lee S, Lim J, Kim C. Tunable fluorescent dendron-cyclodextrin nanotubes for hybridization with metal nanoparticles and their biosensory function. *Angew Chem Int Ed Engl*. 2008; 47: 9922-9926.
  - Qiao Y, Lin Y, Wang Y, Yang Z, Liu J, Zhou J, et al. Metal-driven hierarchical self-assembled one-dimensional nanohelices. *Nano Lett*. 2009; 9: 4500-4504.
  - Zhang X, Tamhane K, Bera T, Fang, JY. Transcription of pH-sensitive supramolecular assemblies into silica: From straight, coiled, and helical tubes to single and double fan-like bundles. *J. Mater. Chem.* 2011; 21: 13973-13977.
  - He C, Shimizu Y, Koshizaki N, Shimizu T. Fluorescent nanotubes consisting of CdS-embedded bilayer membranes of a peptide lipid. *Adv. Mater.* 2007; 19: 1055-1058.
  - Chattopadhyay T, Kogiso M, Asakawa M, Schimizu T, Aoyagi M. Copper (II)-coordinated organic nanotube: A novel heterogeneous catalyst for various oxidation reactions. *Catal. Commun.* 2010; 12: 9-13.
  - Chattopadhyay T, Kogiso M, Aoyagi M, Yui H, Asakawa M, Schimizu T. Single bilayered organic nanotubes: anchors for production of a reusable catalyst with nickel ions. *Green Chem.* 2011; 13: 1138-1140.
  - Terech P, Talmon Y. Aqueous suspensions of steroid nanotubes: Structural and rheological characterizations. *Langmuir*. 2002; 18: 7240-7244.
  - Terech P, Velu SKP, Pernot P, Wiegart L. Salt effects in the formation of self-assembled lithocholate helical ribbons and tubes. *J. Phys. Chem. B* 2012; 116: 11344-11355.
  - Pal A, Basit H, Sen S, Aswal VK, Bhattacharya SJ. Structure and properties of two component hydrogels comprising lithocholic acid and organic amines. *J. Mater. Chem.* 2009; 19: 4325-4334.
  - Zhang X, Zou J, Tamhane K, Kobzeff FF, Fang J. Self-assembly of pH-switchable spiral tubes: supramolecular chemical springs. *Small*. 2010; 6: 217-220.
  - Tamhane K, Zhang X, Zou J, Fang JY. Assembly and disassembly of tubular spherulites. *Soft Matt*. 2010; 6: 1224-1228.
  - Song S, Feng L, Song A, Hao J. Room-temperature super hydrogel as dye adsorption agent. *J. Phys. Chem. B* 2012; 116: 12850-12856.
  - Zhang X, Mathew M, Gesquiere AJ, Fang JY. Synthesis of fluorescent composite tubes with pH-controlled shapes. *J. Mater. Chem.* 2010; 20: 3716-3721.
  - Bera T, Fang JY. Self-assembled palladium-organic composite nanofibers and their applications as a recyclable catalyst. *RSC Adv.* 2013; 3: 21576-21581.